



Published in final edited form as:

Proc SPIE Int Soc Opt Eng. 2023 February ; 12468: . doi:10.1117/12.2654446.

Oxygenation imaging in deep tissue with X-Ray luminescence computed tomography (XLCT)

Yibing Zhang¹, Yile Fang¹, Vigjna Abbaraju², Sriparna Bhattacharya², Jeffrey N. Anker^{2,3}, Ge Wang⁴, Changqing Li^{1,*}

¹Department of Bioengineering, University of California, Merced, Merced, CA 95343, USA.

²Department of Chemistry, Clemson University, Clemson, SC 29634, USA.

³Department of Bioengineering, Center for Optical Materials Science and Engineering Technology (COMSET), and Institute of Environment Toxicology (CU-ENTOX), Clemson University, Clemson, SC 29634, USA.

⁴Department of Biomedical Engineering, Biomedical Imaging Center, Center for Biotechnology and Interdisciplinary Studies, Rensselaer Polytechnic Institute, Troy, NY 12180, USA.

Abstract

Oxygenation concentration of tissue is an important factor in culturing stem cells and in studying the therapy response of cancer cells. The hypoxia bone marrow is the site to harbor cancer cells. Thus, direct high-resolution measurements of molecular O_2 would provide powerful means of monitoring cultured stem cells and therapied cancer cells. We proposed an imaging approach to measure oxygenation concentration in deep tissues, based on the XLCT, with combined strengths of high chemical sensitivity and high spatial resolution. We have developed different biosensing films for oxygenation measurements and tested these films with X-ray luminescent experiments. We have also performed phantom experiments with multiple targets to validate the XLCT imaging system with measurements at two channels.

Keywords

oxygenation; X-ray luminescence; deep tissues; XLCT

1. Introduction

Oxygenation concentration of tissues is an important factor in culturing stem cells and in studying the therapy response of cancer cells. Bone marrow is a typical example of heterogenous hypoxia site [1] where the adult stem cells are maintained. The hypoxic bone marrow is also the site to harbor cancer cells. However, the oxygenation concentration is very heterogenous in tissues like bone marrow and tumors. Thus, direct high-resolution measurements of molecular oxygen (O_2) would provide powerful means of providing insight into the conditions needed to successfully culture stem cells outside of the body and

*Corresponding Author: Changqing Li, Tel.: (209) 228-4777; cli32@ucmerced.edu.

for monitoring the effectiveness of therapeutics. Current available technologies, including SPECT [2], PET [3], and BOLD/TOLD MRI [2][4], have limited spatial resolution of about ~1mm. Although two-photon phosphorescence lifetime microscopy (2PLM) can provide better resolution at micrometer scale, the poor penetration of the visible light (200–500 μm) limits the possibilities of many pre-clinical/clinical applications [5].

In this work, we proposed an imaging approach to measure the oxygenation concentration in deep tissues, based on the XLCT system [6–13], with the combined strengths of high measurement sensitivity and high spatial resolution. The proposed method measures the oxygen concentration by exciting X-ray scintillators which emits optical photons to excite oxygen-dependent phosphorescence dyes [14]. By taking measurements at two different wavelengths, XLCT can image the oxygenation concentrations which depends on the measurement ratio at these two wavelengths. For targets in deep tissues up to several centimeters, we can achieve a spatial resolution of about the superfine x-ray beam size (20 μm). In this study, we have performed the spectrum measurement with various phosphor films at different oxygen concentrations. We have also developed a novel method to reconstruct the complex XLCT targets to increase the quality of the reconstructed XLCT images substantially. This approach has been validated with numerical simulations and phantom experiments.

2. Method

2.1. Biosensing film for oxygenation measurement

To measure the oxygen concentration, we introduced the biosensing films. Figure 1 depicts the design schematic of a typical biosensing film. When X-ray photons excite the scintillator film, a portion of the emitted optical photons from the excited scintillators excite O_2 fluorescence dyes inside the oxygenation indicator film, which is quenched by molecular oxygen.

2.2 X-ray luminescent experimental setup for oxygenation measurement

Figure 2(a) depicts the schematic of the X-ray luminescent experimental system to measure oxygenation concentrations. Figure 2(b) are two photos of the experimental setup. We inserted four different biosensing films inside bone marrow of four different bones (mice leg). As shown in Figure 2(b), the bone samples with biosensing films were then placed inside a cuvette filled with deionized water. We have also inserted an oxygenation probe with an oxygenation meter (Ox-NP, UNISENSE) to monitor the oxygenation of the solution in real time during our measurement for cross validation purpose. A collimated x-ray beam was used to excite the film by aiming the bone. The emitted optical photons were collected by a bifurcated fiber bundle. The two fiber bundles were filtered with two different bandpass filters so that we can calculate the signal ratio at two different wavelengths. The filtered photons were delivered to two PMTs (H7422P-40, H7422P-40, Hamamatsu), pre-amplifier, and then recorded by both a multiple channel photon counter (SR400, SRS) and an oscilloscope (MDO3104, Tektronix). Each measurement photon will generate a single electrical pulse which can be counted by the photon counter. The number of these peaks during a short measurement period were used to calculate the ratios. Table 1 lists the

four films and their corresponding bandpass optical filters. In the filters' names, the number following FB is the central wavelength and the second number indicates the bandwidth.

The X-ray tube was operated at a voltage of 30 kV and a tube current of 0.5 mA. The X-ray beam size was 100 micrometers, and the x-ray excites the film inside the bone samples. The gain of PMTs was set to 0.7. The number of captures from the photon counter for each measurement was 60. The sampling time interval was 1 s and the recorded time window was 0.1 s. The oscilloscope recorded 100,000 data points per capture, which included background and signal pulses.

2.3 XLCT imaging system with multichannel and phantoms with multiple targets

Figure 3 shows photos of the XLCT imaging systems with two measurement fiber bunders. The XLCT imaging system has been described in other publications [6–13]. Briefly, an X-ray tube (X-Beam Powerflux [Mo anode], XOS) was operated at 30 KVp and 0.5 mA with the beam diameter of 100 μm . The object was mounted on the top of a motorized rotary stage (RT-3, Newmark Systems Inc.) which was mounted on a motorized vertical stage (VS-50, Newmark Systems Inc.) and then on a motorized linear stage (NLE-100, Newmark Systems Inc.). The X-ray beam focal spot was at the rotary stage center and was 44.5 mm away from the X-ray lens. As shown in Figure 3b, we used two fiber bundles to measure the emitted optical photons at two spots. And these two fiber bundles were moved together with the object. In this study, we scanned 180 degrees with 6 angular projections and the angular step size of 30 degrees. For each angular projection, a linear scan was performed with 120 steps and the step size of 0.1 mm. We only scan one transverse section. More transverse sections will be scanned in the future.

The water cylindrical phantom has a diameter of 12 mm and a height of 20 mm and was fabricated using 2% agar and 1% intralipid. In the multitargets experiments, glass capillary tubes (standard glass capillaries, WPI) were used as targets. These tubes had an outer diameter of 1mm and an inner diameter 0.58 mm. These tubes were filled with a solution of $Gd_2 O_2 S: Eu^{3+}$ (UKL63/UF-R1, Phosphor Tech. Ltd.) at a concentration of 10 mg/mL. The targets were vertically embedded within the background phantom. In this paper, three different target cases were studied: one target, two targets, and three targets. For experiments involving multiple targets, the glass capillary tubes were arranged side by side in order to simplify the image analysis of the reconstruction results.

During the experiment, the fibers were positioned close to the phantom in order to increase photon collection efficiency. The photons were collected by the fiber bundles and then delivered to photomultiplier tubes (PMTs) (H7422-40, Hamamatsu). The output signals from the PMTs were amplified using a broadband amplifier (SR455A, Stanford Research Systems) with a gain factor of 125 and filtered by a low-pass filter (BLP-10.7+, cutoff frequency of 11 MHz, Mini-Circuits). Then the filtered signals were recorded by a two-channel photon counter (SR400, Stanford Research Systems) for the XLCT reconstruction algorithm [10–12]. The XLCT imaging system was controlled by a lad-made code.

3. Result

3.1 Measured emission spectrum

Figure 4 plots the measured emission spectrum of the oxygenation sensing film PtPP. From this figure, we see that the emission peaks and their ratios are changed at different oxygenations. These changes will be used for us to sense the oxygenation in deep tissues.

3.2 Oxygenation measurement results

The measured results are shown in figure 5. Figure 5 (a) depicts a typical oscilloscope screen during the measurement, in which the pulses of the two channels in the oscilloscope window are indicators of the measured optical photons. These pulses were also recorded by the two-channel photon counter. We measured four films as listed in Table 1. All four films showed the ratio change due to the changed oxygen concentrations of the solution inside the cuvette. Figure 5 (b) plots the photon number ratio for the film of Y2O2S-Tb_PtTFPP at oxygen concentration 14% and 0%, respectively. When the oxygenation was at 14% and 0%, the ratio of measurement was calculated to be 2.95 and 1.161, respectively.

3.3 Results of phantom experiments

The reconstructed XLCT images are plotted in Figures 6(a) and 6(b) for one target case, Figures 6 (c) and 6 (d) for two targets case, and Figures 6 (e) and 6(f) for three targets cases, respectively. Figures 6(b), 6(d) and 6(f) are zoomed in for image analysis. The scan depth for all three cases was 5 mm below the top surface.

Fig. 6(a) plots the reconstructed XLCT image for one target case and Fig. 6(b) is the zoomed in image around the target. The inner diameter of the target is 0.58 mm. The calculated target size is about 0.5871 as indicated in Fig. 6(b), which is very close to the ground truth. Fig. 6(c) plots the reconstructed XLCT imaging for two targets case and Fig. 6(d) is its zoomed in image around the two targets. From Fig. 6(d), we measured the edge-to-edge distance to be 0.515 mm. The two targets were placed close to each other. Each target has an outside diameter of 1 mm and an inside diameter of 0.58mm. Thus, the true edge-to-edge distance is 0.42 mm. From Fig. 6(d), we see that the reconstructed target sizes are very close to the true target size. Fig. 6(e) plots the reconstructed XLCT image for three target cases. Fig. 6(f) is its zoomed in figure around the three targets. From Fig. 6(f), we found that the inter-target distances were 0.445 mm and 0.456 mm, respectively. The average error of the edge-to-edge distances for two targets and three targets cases is estimated to be 12.26%.

We also found that the reconstructed value of the inner target is less than the outside target, which may be caused by the X-ray beam intensity attenuations. In our reconstruction, we have not included the X-ray intensity attenuation. This factor should be included in the future XLCT reconstruction for better quantitative results. In this experiment, we only scanned the object 180 degrees, which may result in some quantitative errors. In future, we will scan the object 360 degrees and add more angular projections for better XLCT image quality.

In this experiment, we have not used the bandpass optical filters for multiple wavelength measurements. In the future, we will bifurcate fiber bundles to measure photons at two different wavelengths simultaneously at the same measurement spot so that we can calculate the emission ratios for oxygenation extraction in deep targets.

4. Conclusions

In this work, we have proposed an XLCT system based method to measure oxygenation concentrations in deep tissue study. We successfully have used biosensing films to observe significant ratio changes when the oxygenation concentration changes from 14% to 0%. We have performed XLCT imaging experiments with measurements from two optical fiber bundles and have successfully reconstructed all cases including three targets case. The average error of the reconstructed edge-to-edge distances are 12.26%.

In the future, we will use an X-ray tube with super fine beam, as shown in Figure 7(a), from Sigray Inc. The X-ray beam diameter is as small as 20 μm . In this design, we will use a 3d rotary stage and 8 PMTs to achieve fast scanning, better spatial resolution, and 3d imaging capability for vivo mice study. The 3D design of the proposed XLCT system is shown in Figure 7(b).

Acknowledgement

This work was partially funded by the National Institute of General Medical Sciences (NIGMS) [R42GM142394-01A1] and National Institute of Biomedical Imaging and Bioengineering (NIBIB) [R01EB026646].

Reference

- [1]. Clark DP, & Badea CT (2014). Micro-CT of rodents: state-of-the-art and future perspectives. *Physica medica : PM : an international journal devoted to the applications of physics to medicine and biology : official journal of the Italian Association of Biomedical Physics (AIFB)*, 30(6), 619–634. [PubMed: 24974176]
- [2]. Davda S, Bezabeh T. Advances in methods for assessing tumor hypoxia in vivo: Implications for treatment planning. *Cancer Metastasis Rev.* 2006 Dec 6;25(3):469–480. [PubMed: 17029029]
- [3]. Grkovski M, Schöder H, Lee NY, Carlin SD, Beattie BJ, Riaz N, Leeman JE, O'Donoghue JA, Humm JL. Multiparametric imaging of tumor hypoxia and perfusion with 18 F-fluoromisonidazole dynamic pet in head and neck cancer. *J Nucl Med.* 2017 Jul;58(7):1072–1080. [PubMed: 28183993]
- [4]. Hiraga T Hypoxic microenvironment and metastatic bone disease. *Int J Mol Sci.* 2018 Nov;19(11):3523. [PubMed: 30423905]
- [5]. Spencer J, Ferraro F, Roussakis E et al. Direct measurement of local oxygen concentration in the bone marrow of live animals. *Nature* 508, 269–273 (2014). [PubMed: 24590072]
- [6]. Zhang Wei, Lun Michael, Nguyen Alex Anh-Tu, Li Changqing “A focused x-ray beam based x-ray luminescence computed tomography”, *Journal of Biomedical Optics*, 22(11), 116004 (2017). [PubMed: 29127693]
- [7]. Wei Zhang W, Zhu Dianwen, Lun Michael, Li Changqing, “Collimated superfine x-ray beam based x-ray luminescence computed tomography”, *Journal of X-ray Science and Technology*, 25(6), 945–957 (2017). [PubMed: 28598861]
- [8]. Lun MC, Cong WX, Arifuzzaman M, Ranasinghe M, Bhattacharya S, Anker JN, Wang G, Li CQ, “Focused x-ray luminescence imaging system for small animals based on a rotary gantry”, *Journal of Biomedical Optics*, V26 (3), 036004 (2021).

- [9]. Zhang YM, Lun M, Li CQ, Zhou ZX, “Method for improving the spatial resolution of narrow x-ray beam-based x-ray luminescence computed tomography imaging”, *Journal of Biomedical Optics*, 24(8), 086002 (2019). [PubMed: 31429215]
- [10]. Zhu Dianwen, Li Changqing, “Nonconvex regularizations in fluorescence molecular tomography for sparsity enhancement”, *Physics in Medicine and Biology*, 59, 2901 (2014). [PubMed: 24828748]
- [11]. Zhu Dianwen, Li Changqing, “Accelerated image reconstruction in fluorescence molecular tomography using a nonuniform updating scheme with momentum and ordered subsets methods”, *Journal of Biomedical Optics*, 21(1), 016001 (2016).
- [12]. Zhu Dianwen, Li Changqing, “Nonuniform update for sparse target recovery in fluorescence molecular tomography accelerated by ordered subsets”, *Biomedical Optics Express*, 5, 4249–4259 (2014). [PubMed: 26623173]
- [13]. Fang Yile, Lun Michael C., Zhang Yibing, Anker Jeffrey N., Wang Ge, Li Changqing, “Superfast three-dimensional focused x-ray luminescence computed tomography with a gated photon counter,” *Proc. SPIE 12036, Medical Imaging 2022: Biomedical Applications in Molecular, Structural, and Functional Imaging*, 120360K (4 April 2022);
- [14]. Uzair U, Johnson C, Beladi-Behbahani S, Rajamanthrilage AC, Raval YS, Benza D, Ranasinghe M, Schober G, Tzeng TJ, Anker JN. Conformal Coating of Orthopedic Plates with X-ray Scintillators and pH Indicators for X-ray Excited Luminescence Chemical Imaging through Tissue. *ACS Appl Mater Interfaces*. 2020 Nov 25;12(47):52343–52353. doi: 10.1021/acsami.0c13707. [PubMed: 33181017]

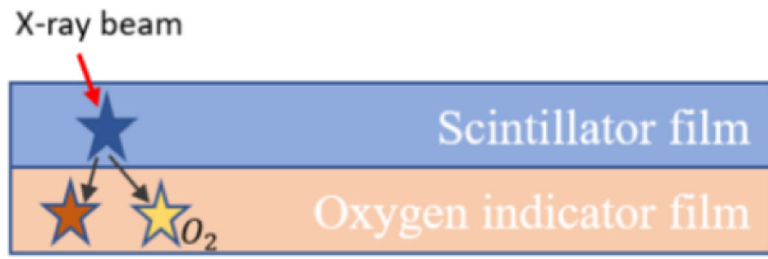


Figure 1.
Sensor schematic and mechanism

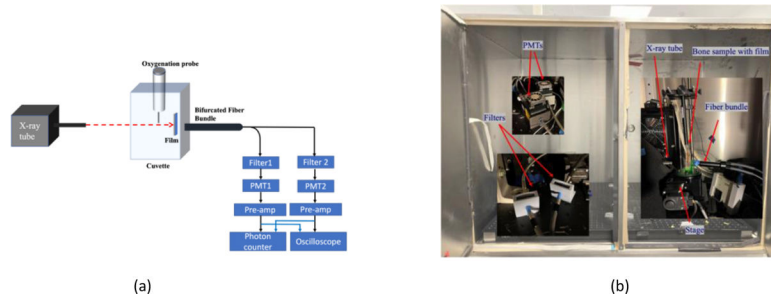


Figure 2.
(a) Schematic of X-ray luminescent measurement setup; (b) Photos of the experiment system

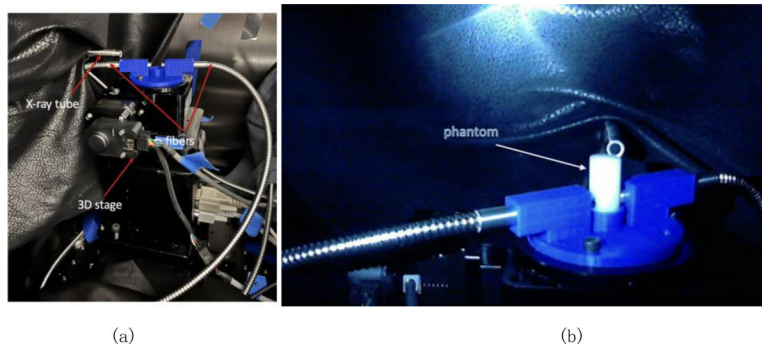


Figure 3.
(a) XLCT imaging system; (b) Phantom with two fiber bundles on the top of the rotary stage.

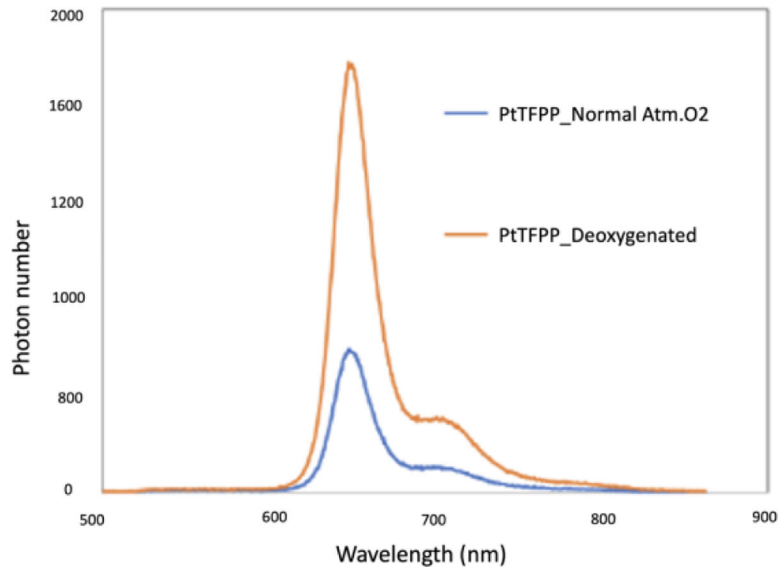
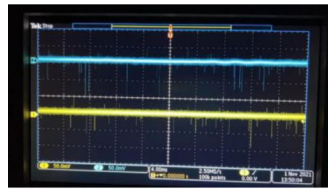
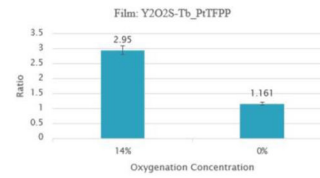


Figure 4.
Emission spectrum of PtPP patch under different oxygen concentrations.



(a)



(b)

Figure 5.

(a) Screen shot of a typical oscilloscope measurement, where the pulses are indicators of the emitted optical photons; (b) Photon number ratio for the film of Y2O2S-Tb_PtTFPP at different oxygenation concentrations.

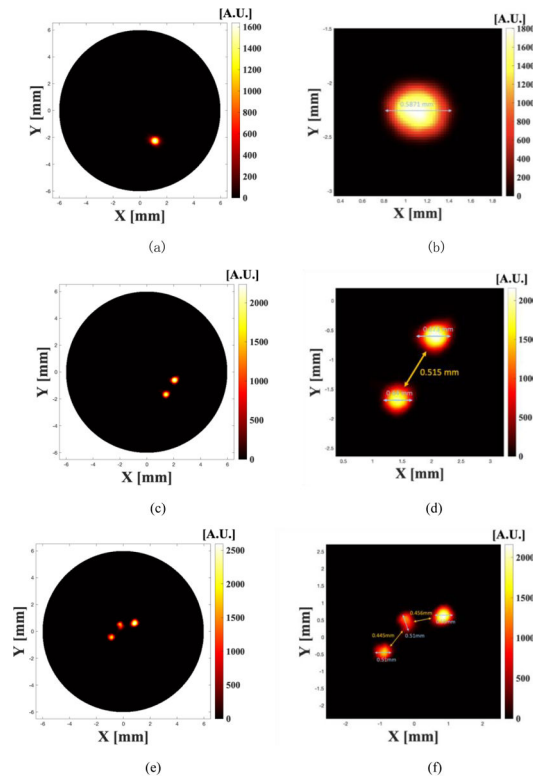


Figure 6. Reconstructed XLCT images from phantom experiments for the one target case (a, b), two targets case (c, d), and three targets case (e, f). Figures (b, d, f) are the zoomed in images around the reconstructed targets.

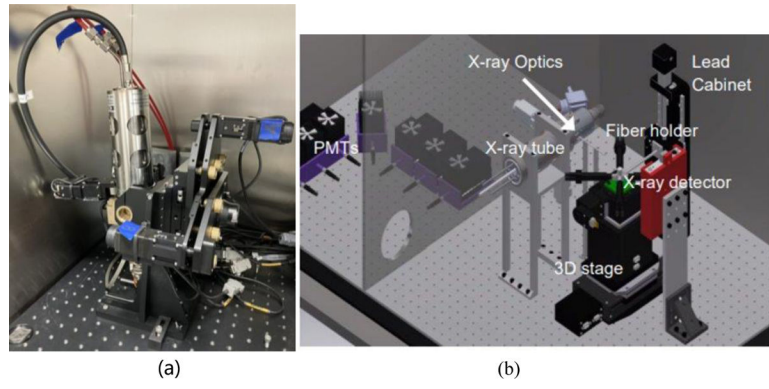


Figure 7. (a) X-ray tube form Sigray with 20 μm beam size; (b) prototype of CAD 3D design XLCT system.

Table 1.

The films and their corresponding filters

Film Name	Channel A Filter	Channel B Filter
Gd202sTb_PtOEPk	FB680-40	FB750-40
Lu2SiO5Ce_PtTFPP	FB680-40	FB650-40
SrAl2O4:Eu_PtTFPP	FB680-40	FB650-40
Y2O2S-Tb_PtTFPP	FB680-40	FB650-40

Author Manuscript

Author Manuscript

Author Manuscript

Author Manuscript